# Application-oriented analysis of material interface reconstruction algorithms in time-varying bijel simulations

X. Bao[1], N. Karthikeyan[2], U. D Schiller[2], F. Iuricich[1]

[1]School of Computing, Clemson University, United States
[2]Department of Material Science, Clemson University, United States

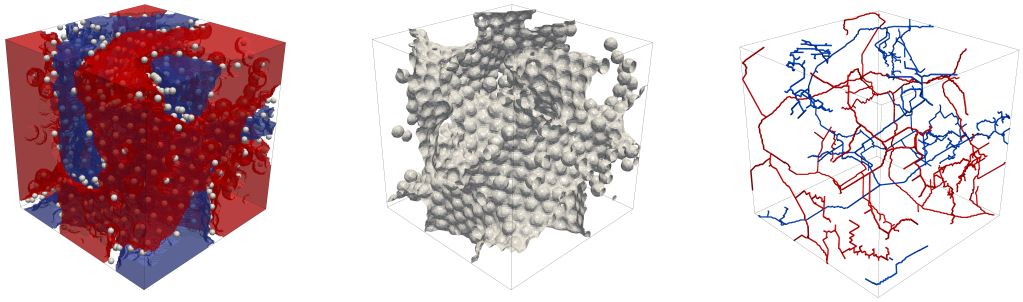

(a) (b) (c)

**Figure 1:** *A multimaterial dataset is typically represented by a multivariate function defined on the cells of a cubical grid. In this paper, we use a bijel simulation dataset composed of oil and water with the addition of particles animated with the fluid to study the fluid-particle interactions. Bijels are tortuous microscopic structures formed by stabilizing the interface of two fluids. (a) Cells of the discrete domain can either contain oil (red), water (blue), or a mix of the two. Particles in the simulation, depicted as gray spheres, influence the formation of the bijel. Multimaterial interface reconstruction is a well-known problem in multimaterial analysis which involves (b) identifying the surface separating the two materials. To analyze the characteristics of a multimaterial domain scientists need geometric structures beyond the interface. One of these is the medial axies, (c) here representing the topological skeletons of the oil (red) and water (blue) components.*

**Abstract**

*Multimaterial interface reconstruction has been investigated over the years both from visualization and analytical point of view using different metrics. When focusing on visualization, interface continuity and smoothness are used to quantify interface quality. When the end goal is interface analysis, metrics closer to the physical properties of the material are preferred (e.g., curvature, tortuosity). In this paper, we re-evaluate three Multimaterial Interface Reconstruction (MIR) algorithms, already integrated in established visualization frameworks, under the lens of application-oriented metrics. Specifically, we analyze interface curvature, particle-interface distance, and medial axis-interface distance in a time-varying bijel simulation. Our analysis shows that the interface presenting the best visual qualities is not always the most useful for domain scientists when evaluating the material properties.*

**CCS Concepts**

• ***Computing methodologies*** → ***Volumetric models;*** • ***Human-centered computing*** → ***Scientific visualization;***

## 1. Introduction

An important component of multi-material simulation analysis is the computation of the interface. Intuitively, reconstructing a multi-material interface means to construct a surface that separates materials within each cell of the domain. Studying the shape, topology, and cavities of the interface allows to derive important information about the material under study [MTB*19]. To this end, Material Interface Reconstruction (MIR) algorithms have received a considerable amount of attention in computational physics [Cam21],



DOI: 10.2312/evs.20221104

computer graphics [AGDJ08], scientific visualization [AGDJ10], and material science [WLWH12].

However, approaches developed by different communities have been evaluated with different criteria. Broadly speaking, we can classify MIR techniques as either simulation-oriented or visualization-oriented. The firsts focus on physical properties such as mass convergence [NP17] and flux volume [KSM*13]. The seconds focus on the quality of the produced mesh [OCHJ12], or memory consumption and run time performance [MC10].

This paper provides two novelties in the analysis of MIR algorithms. First, we provide an application-oriented evaluation of several MIR algorithms integrated in existing scientific visualization frameworks (e.g., VisIt [Chi12], ParaView [Aya15]). Second, we analyze the results consistency by considering the full time-varying evolution of the bijel interface rather than a single time step.

## 2. Background and Related Work

Multimaterial analysis generally starts from a *simulation method* used to create a discrete multimaterial description. In this work we used a *Lattice Boltzmann Method (LBM)*, a relatively new simulation technique that can be seen as a mixture of particle-based (e.g., Lagrangian [GM77]), and mesh-based approaches (e.g. Eulerian [TP03]). LBM is often used in porous media simulations due to its ability to capture complex boundaries and microscopic interactions [JH11]. The output of a LBM model is a multivariate function $f : \mathcal{D} \longrightarrow \mathbf{R}$, defined on the cells of a cubical grid $\mathcal{D}$.

Given $f$, *Multimaterial Interface Reconstruction (MIR)* computes a mesh $\mathcal{M}$ describing the material boundaries. Ideally, we subdivide each cell of $\mathcal{D}$ such that the total volume of each material within the cell equals the materials volume fraction. The difference between the original materials volume fraction and the volumes obtained by subdividing the cell according to $\mathcal{M}$ defines the *volume accuracy* [MC10]. The most straightforward and earliest method to reconstruct the interface is the Simple Line Interface Calculation (SLIC) [NW76], which uses axis-aligned planes to partition cells according to the material fraction volume. To improve the geometric quality of the reconstructed interface, Piecewise Linear Interface Calculation (PLIC) [You84] methods generalize the SLIC approach by allowing lines/planes with arbitrary orientations. These can be defined based on the finite-difference on the volume fraction grid [HN81], the gradient of the volume fraction grid [You84], or by solving a least square problem [Puc91].

SLIC and PLIC methods have the advantage of speed and simplicity. The drawback is that they compute independent geometries for each material, which are generally disconnected. Reconstructing an interface with correct topology is a challenging problem [MC10, AGDJ10]. For a two-material scenario, Meredith et al. [Mer05] addressed this problem by first averaging volume fraction values at the cells' vertices. Then, the interface is obtained by computing the isosurface for the isovalue 0.5. Notice that with two materials, we are under the assumption that the sum of volume fractions is always 1. Thus, the volume fraction of both materials generate the same isosurface.

Anderson et al. [AGDJ08, AGDJ10] introduced the idea to subdivide cells into a discretized grid and iteratively swap sub-cell materials to minimize an energy function. This approach can guarantee bounded errors for the reconstructed surface but has the disadvantage of being memory and time-consuming.

## 3. MIR Algorithm comparison

We compare three MIR algorithms widely adopted in the visualization community; namely, EquiT and EquiZ both proposed by Meredith et al. [Mer05], and Discrete proposed by Anderson et al. [AGDJ08]. All these methods are implemented in the VisIt framework. Notice that while PLIC [You84] is provided by both ParaView [Aya15] and VisIt [Chi12], here we do not include PLIC in our analysis since it does not provide an interface as output.

The dataset we use in our comparison is the simulation of a time-varying bicontinuous interfacially jammed emulsion gel (bijels).

Loosely speaking, bijels are tortuous microscopic structures formed by stabilizing the interface of two fluids [HWS*07]. A bijel interface is similar to the mathematical surface called gyroid [MTB*19, RST16], whose characteristics are beneficial for material diffusivity and conductivity. The dataset is produced by LB3D [SSF*17], a multi-component, multi-phase solver for LBM methods. LB3D manipulates the density fields of the two fluids simulating the interface tension between the fluids [JH11]. In our data set, two fluids are randomly dispersed within a $256^3$ cube with spherical particles with a radius of 5 voxels (see Figure 1a). The volume fraction data of two fluids are produced for 28 snapshots taken periodically in the 30000 simulation timesteps. Since Discrete required more than 64GB of memory (the limit for our system) to reconstruct the interface on the original dataset, we cropped the original dataset at its center within a $128^3$ window. The interface quality is evaluated using four different metrics related to geometric characteristics of the multimaterial, namely interface's Gaussian and Mean curvature, particles to interface distance, and medial axis to interface distance.

### 3.1. Evaluating interfaces with curvature estimators

Surface curvature is the most broadly used property in mesh quality estimation. Surface curvatures are defined based on two principal curvatures, $k_1$ and $k_2$, which indicate how the surface bends in the two principal directions at that point. The Gaussian curvature is defined as the product of the two principal curvatures, while Mean curvature is the average value of the two [HEZ*19, Por94]. A bijel-derived interface should display similar features of a gyroid, characterized by 0 Mean Curvature and negative Gaussian Curvature. Thus, an ideal result from the curvature analysis should show similar statistics [MTB*19].

Gaussian and Mean curvature values are generally estimated at the vertices of a mesh [Por94]. This operation can be challenging in the presence of non-manifold vertices. In our evaluation, we used the approach proposed by [CSM03], which estimates the curvature in a small neighborhood of a given vertex. We computed Mean and Gaussian curvature on the interfaces extracted from all 28 snapshots by each of the three methods. For each interface, curvature values are computed on 10000 vertices sampled over the interface mesh.

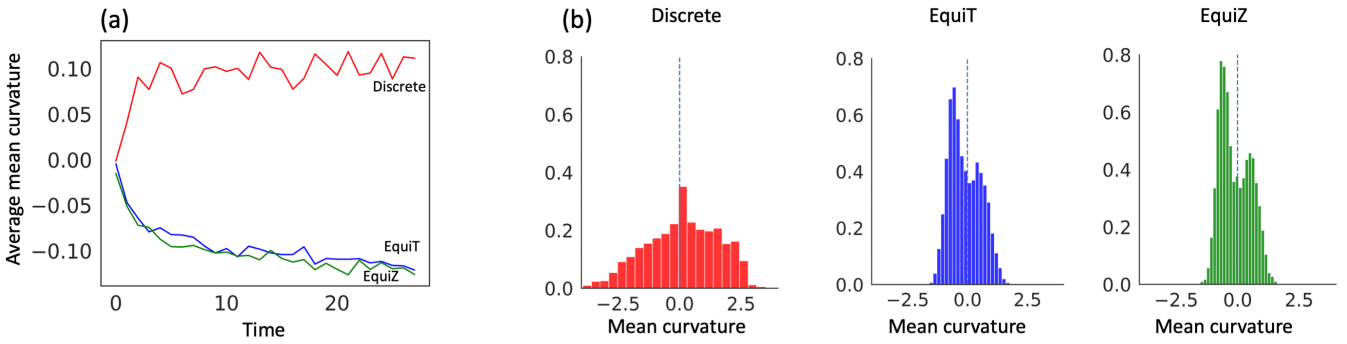


**Figure 2:** *(a) Average Mean Curvature as a function of time. for Discrete (red), EquiT (blue), and EquiZ (green). (b) Mean Curvature distribution for a representative snapshot of the simulation.*

**Mean curvature analysis** Figure 2a shows the average mean curvature value computed for each snapshot of the simulation. We can observe an early variation in the average Mean curvature. The phenomenon is due to drastic changes in the interface topology [JH11] that, after 2 snapshots, remains stable until the end of the simulation. We can notice that Discrete, EquiT, and EquiZ align differently to the expected results (average of Mean curvature equal to 0). In particular, the Discrete method tends to produce positive values while EquiT and EquiZ tend to produce negative values.

Figure 2b shows the distribution of mean curvature values computed on the three interfaces for a representative snapshot (i.e., 10). These confirm the trends seen in Figure 2a since the Discrete method tends to have more positive values while EquiT, and EquiZ tend to have more negative values. Interestingly, the three algorithms show different distributions. EquiT and EquiZ show a bimodal distribution, while Discrete shows a unimodal distribution. Overall, EquiT and EquiZ show curvature values closer to zero, which indicate they better align to the expected characteristics of a minimal surface structure [RST16]. This also suggests that EquiT and EquiZ produce a smoother interface than Discrete, whose curvature values have more variation.

**Gaussian curvature analysis** Figure 3a shows the average Gaussian curvature values obtained on each snapshot for the three methods. We can notice that on average, only Discrete and EquiT produce overall negative values while the average Gaussian curvature of the interface computed by EquiZ assumes positive values. Interestingly, while EquiZ and EquiT both use a similar strategy to compute the interface, the tetrahedral-based subdivision used by EquiT seems beneficial for Gaussian curvature estimation. Figure 3b shows a detailed view of the distribution of the Gaussian values using histograms, which confirms the general trends seen in the line chart. Notice that only a few values are obtained on the interface computed with the Discrete method since, similarly to SLIC [NW76], this approach reconstructs axis-aligned boundaries between voxels.

Overall, we should mention that curvature analysis presents challenges with all these methods due to small artifacts in the reconstructed interfaces. In the case of bijels analysis, this may come from contact points between spherical pockets corresponding to the original particles used by the simulation (see Figure 1b). From a domain scientist's perspective, this problem underlines the need for numerically robust, other than visually accurate, MIR algorithms.

### 3.2. Evaluating interfaces with particle-surface distance

Particle-interface contact angle is one parameter of the LB3D simulation that describes the particle wettability of two fluids [JH11]. Particles accumulate at the interface during the bijels evolution [JH11]. Then, we expect the particle-interface distance to decrease over time.

Figure 4a shows the average distance values computed for each snapshot. We notice that the average particle distance increases over time, and the same trend is visible for all interfaces. This contradicts the expectation that particles converge to the interface over time [JH11]. The hypothesis is that all these approaches are actually failing to capture thin interfaces formed around small droplets (particles) away from the "main" interface. To test this hypothesis, we quantified the number of expelled particles which is shown in Figure 4b. These are particles at distances more than twice the average particle-interface distance. From Figure 4b we notice that the number of such particles increases over time. Particles cannot be expelled since it is energetically unfavorable for the simulation [JH11], the result indicates that parts of the interface are being omitted. In other words, all these approaches still have inaccurately reconstructed interfaces for small droplets.

### 3.3. Medial Axis and Material-Interface Distance

The medial axis [BLU67] is a topological skeleton, formed by edges and vertices, used to describe complex morphology. Medial axis is widely used in many areas, including path planning [WAS99], pattern recognition [SK05] and shape analysis [SCYW16]. In material science, the medial axis of a material volume is used to estimate physical properties of porous media such as domain size and tortuosity [MTB*19]. In the case of bijels analysis, we have two medial axes (one per material), and we are interested in investigating their relations with the interface extracted from each MIR algorithm. Given the fact that the two material volume fractions are equal during the entire simulation, we expect the interface to be (on average) equidistant from both material's medial

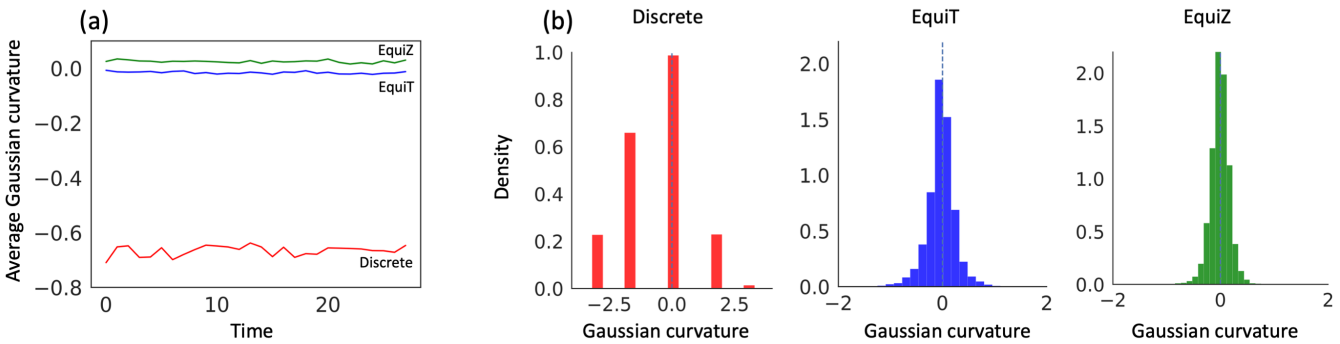


**Figure 3:** *(a) Average Gaussian Curvature as a function of time for Discrete (red), EquiT (blue) and EquiZ (Green). (b) Gaussian Curvature distribution for a representative snapshot of the simulation.*

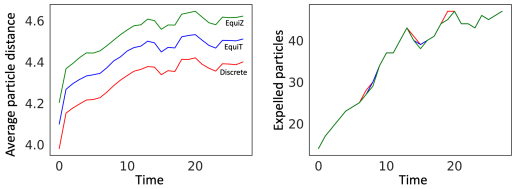


**Figure 4:** *Average particle interface distance (a) and number of Expelled particle (b) as a function of time with Discrete (red), EquiT (blue), and EquiZ (green). Each particle is classified as expelled particle if its distance from the interface is larger than twice the average particle-interface distance.*

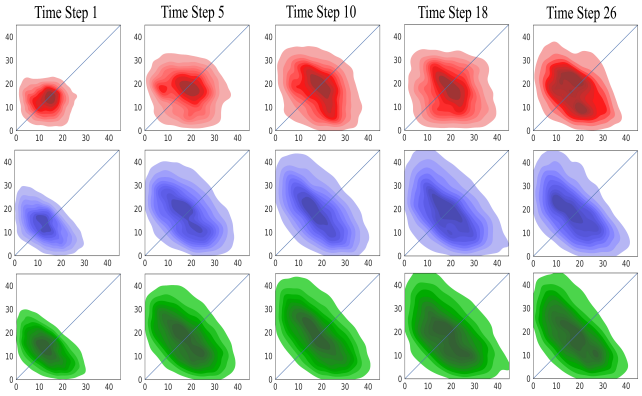


**Figure 5:** *Co-variate distribution of the interface vertices distance from the two medial axis. For each density plot, X-axis represents the distance of a point in the interface from the medial axis of the oil material; Y-axis represents the distance of the point from the medial axis of the water material.*

axis. To test this hypothesis we first compute the medial axis using the Teasar algorithm [SBB*00] on each material. Then, for each vertex on the interface, we compute its distance to the closest point on each medial axis.

Figure 5 shows the distribution of the results obtained. The figure is created by embedding each vertex $p$ of the interface in a 2D space. The coordinates of $p$ are defined by the vertex's distance from the oil medial axis (X-coordinate) and the water medial axis (Y-coordinate). Then, we compute a Kernel Density Estimation (KDE) from the point cloud to show the co-variate distribution of the interface distances.

We can notice that all distributions are symmetric and centered on the diagonal. This means that all interfaces reconstructed are roughly equidistant from both medial axes. However, if we look at the results over time (left to right), we see that all distributions move up along the diagonal and occupy a larger area towards the end of the simulation with respect to the beginning. This is the effect of smaller droplets being merged into the two material volumes, which results in the two medial axes being pushed away from the interface. At the same time, if we compare the three results for the same time step, we can notice that the distribution obtained by the Discrete method occupies smaller regions compared to the others. This indicates that EquiT and EquiZ tend to exaggerate this effect by computing interfaces that are unbalanced towards one of the two materials.

## 4. Conclusion

In this paper, we compared three MIR algorithms in terms of interface curvature, particle-interface distance, and interface-material distance using a time-varying bijel simulation. From a visual point of view, EquiZ is considered the approach producing the best interfaces. However, we have shown that each approach presents strengths and weaknesses when evaluating the obtained interface from a quantitative point of view. Our results highlight the need to incorporate application-oriented evaluation metrics in MIR algorithms evaluation to improve MIR accuracy and to help domain scientists in the selection of the most suited MIR algorithm for their end-goal.

## 5. Acknowledgment

This work was supported in part by the US National Science Foundation under award DMR-1944942 and the Clemson R-initiatives. We would like to thank the reviewers for their insightful comments.

## References


[AGDJ08] ANDERSON J. C., GARTH C., DUCHAINEAU M. A., JOY K. I.: Discrete multi-material interface reconstruction for volume fraction data. *Computer Graphics Forum 27*, 3 (May 2008), 1015–1022. doi:10.1111/j.1467-8659.2008.01237.x. 2

[AGDJ10] ANDERSON J. C., GARTH C., DUCHAINEAU M. A., JOY K. I.: Smooth, volume-accurate material interface reconstruction. *IEEE Trans. Visual. Comput. Graphics 16*, 5 (Sept. 2010), 802–814. doi:10.1109/TVCG.2010.17. 2

[Aya15] AYACHIT U.: *The ParaView guide: [a parallel visualization application]; updated for ParaView version 4.3$nUtkarsh Ayachit*. Kitware, 2015. 2

[BLU67] BLUM, H.: A transformation for extracting new descriptors of shape. 362–380. 3

[Cam21] CAMPBELL B. K.: An arbitrarily high-order three-dimensional cartesian-grid method for reconstructing interfaces from volume fraction fields. *Journal of Computational Physics 426* (Feb. 2021), 109727. doi:10.1016/j.jcp.2020.109727. 1

[Chi12] CHILDS, HANK: VisIt: An end-user tool for visualizing and analyzing very large data. 2

[CSM03] COHEN-STEINER D., MORVAN J.-M.: Restricted delaunay triangulations and normal cycle. In *Proceedings of the nineteenth conference on Computational geometry - SCG '03* (2003), ACM Press, p. 312. doi:10.1145/777792.777839. 2

[GM77] GINGOLD R. A., MONAGHAN J. J.: Smoothed particle hydrodynamics: theory and application to non-spherical stars. *Monthly Notices of the Royal Astronomical Society 181*, 3 (Dec. 1977), 375–389. doi:10.1093/mnras/181.3.375. 2

[HEZ*19] HSIEH M.-T., ENDO B., ZHANG Y., BAUER J., VALDEVIT L.: The mechanical response of cellular materials with spinodal topologies. *Journal of the Mechanics and Physics of Solids 125* (2019), 401–419. doi:10.1016/j.jmps.2019.01.002. 2

[HN81] HIRT C., NICHOLS B.: Volume of fluid (VOF) method for the dynamics of free boundaries. *Journal of Computational Physics 39*, 1 (Jan. 1981), 201–225. doi:10.1016/0021-9991(81)90145-5. 2

[HWS*07] HERZIG E. M., WHITE K. A., SCHOFIELD A. B., POON W. C. K., CLEGG P. S.: Bicontinuous emulsions stabilized solely by colloidal particles. 966–971. doi:10.1038/nmat2055. 2

[JH11] JANSEN F., HARTING J.: From bijels to pickering emulsions: A lattice boltzmann study. *Phys. Rev. E 83*, 4 (Apr. 2011), 046707. doi:10.1103/PhysRevE.83.046707. 2, 3

[KSM*13] KARCH G. K., SADLO F., MEISTER C., RAUSCHENBERGER P., EISENSCHMIDT K., WEIGAND B., ERTL T.: Visualization of piecewise linear interface calculation. In *2013 IEEE Pacific Visualization Symposium (PacificVis)* (Feb. 2013), IEEE, pp. 121–128. doi:10.1109/PacificVis.2013.6596136. 2

[MC10] MEREDITH J. S., CHILDS H.: Visualization and analysis-oriented reconstruction of material interfaces. *Computer Graphics Forum 29*, 3 (Aug. 2010), 1241–1250. doi:10.1111/j.1467-8659.2009.01671.x. 2

[Mer05] MEREDITH, JS: Material interface reconstruction in VisIt, 2005. 2

[MTB*19] MCDEVITT K. M., THORSON T. J., BOTVINICK E. L., MUMM D. R., MOHRAZ A.: Microstructural characteristics of bijel-templated porous materials. *Materialia 7* (2019), 100393. doi:10.1016/j.mtla.2019.100393. 1, 2, 3

[NP17] NGUYEN V.-T., PARK W.-G.: A volume-of-fluid (VOF) interface-sharpening method for two-phase incompressible flows. *Computers & Fluids 152* (July 2017), 104–119. doi:10.1016/j.compfluid.2017.04.018. 2

[NW76] NOH W. F., WOODWARD P.: SLIC (simple line interface calculation). In *Proceedings of the Fifth International Conference on Numerical Methods in Fluid Dynamics June 28 – July 2, 1976 Twente University, Enschede*, van de Vooren A. I., Zandbergen P. J., (Eds.), vol. 59. Springer Berlin Heidelberg, 1976, pp. 330–340. Series Title: Lecture Notes in Physics. doi:10.1007/3-540-08004-X_336. 2, 3

[OCHJ12] OBERMAIER H., CHEN F., HAGEN H., JOY K. I.: Visualization of material interface stability. In *2012 IEEE Pacific Visualization Symposium* (Feb. 2012), IEEE, pp. 225–232. doi:10.1109/PacificVis.2012.6183595. 2

[Por94] PORTEOUS I. R.: *Geometric differentiation: for the intelligence of curves and surfaces*. Cambridge University Press, 1994. 2

[Puc91] PUCKETT, ELBRIDGE GERRY: A volume-of-fluid interface tracking algorithm with applications to computing shock wave refraction. In *Proceedings of the Fourth International Symposium on Computational Fluid Dynamics*. 1991, pp. 933–938. 2

[RST16] REEVES M., STRATFORD K., THIJSSEN J. H. J.: Quantitative morphological characterization of bicontinuous pickering emulsions *via* interfacial curvatures. *Soft Matter 12*, 18 (2016), 4082–4092. doi:10.1039/C5SM03102H. 2, 3

[SBB*00] SATO M., BITTER I., BENDER M., KAUFMAN A., NAKAJIMA M.: TEASAR: tree-structure extraction algorithm for accurate and robust skeletons. In *Proceedings the Eighth Pacific Conference on Computer Graphics and Applications* (2000), IEEE Comput. Soc, pp. 281–449. doi:10.1109/PCCGA.2000.883951. 4

[SCYW16] SUN F., CHOI Y.-K., YU Y., WANG W.: Medial meshes – a compact and accurate representation of medial axis transform. *IEEE Trans. Visual. Comput. Graphics 22*, 3 (Mar. 2016), 1278–1290. doi:10.1109/TVCG.2015.2448080. 3

[SK05] SEBASTIAN T. B., KIMIA B. B.: Curves vs. skeletons in object recognition. *Signal Processing 85*, 2 (Feb. 2005), 247–263. doi:10.1016/j.sigpro.2004.10.016. 3

[SSF*17] SCHMIESCHEK S., SHAMARDIN L., FRIJTERS S., KRÜGER T., SCHILLER U., HARTING J., COVENEY P.: LB3d: A parallel implementation of the lattice-boltzmann method for simulation of interacting amphiphilic fluids. 149–161. doi:10.1016/j.cpc.2017.03.013. 2

[TP03] TRAC H., PEN U.: A primer on eulerian computational fluid dynamics for astrophysics. *PUBL ASTRON SOC PAC 115*, 805 (Mar. 2003), 303–321. doi:10.1086/367747. 2

[WAS99] WILMARTH S. A., AMATO N. M., STILLER P. F.: Motion planning for a rigid body using random networks on the medial axis of the free space. In *Proceedings of the fifteenth annual symposium on Computational geometry - SCG '99* (1999), ACM Press, pp. 173–180. doi:10.1145/304893.304967. 3

[WLWH12] WEI L., LIN X., WANG M., HUANG W.: A cellular automaton model for a pure substance solidification with interface reconstruction method. *Computational Materials Science 54* (Mar. 2012), 66–74. doi:10.1016/j.commatsci.2011.10.012. 2

[You84] YOUNGS D.: An interface tracking method for a 3d eulerian hydrodynamics code. 2